Front. Earth Sci. 2020, 14(2): 326–343
https://doi.org/10.1007/s11707-019-0775-7

RESEARCH ARTICLE

A spatial model for the assessment of debris flow susceptibility along the Kodaikkanal-Palani traffic corridor

Evangelin Ramani SUJATHA

Centre for Advanced Research on Environment, School of Civil Engineering, SASTRA Deemed University, Thanjavur 613401, India

Abstract Debris flow is one of the most destructive water related mass movements that affects the development of mountain terrains. A reliable assessment of debris flow susceptibility requires adequate data, but in most developing countries like India, there is a dearth of such extensive scientific records. This study presents a novel approach for assessing debris flow using the analytical network process (ANP) in data insufficient regions. A stretch of hill road between Kumburvayal and Vadakaunchi along the Kodaikkanal-Palani Traffic Corridor (M171) was considered for this study. Five significant factors including the nature of slope forming materials, hydraulic conductivity, slope, vegetation, and drainage density were identified from intense field surveys and inspections in order to assess the susceptibility of the terrain to debris flow. This model endorsed the interdependencies between the selected factors. The resulting debris flow susceptibility map delineated regions highly prone to debris flow occurrences, which constituted nearly 23% of the selected road stretch.

Keywords analytical network process (ANP), debris flow, hydraulic conductivity, GIS, Kodaikkanal, infinite slope stability model, steady state hydrologic model

1 Introduction

Debris flow is a common geomorphic hazard that affects the hill and mountain regions of the world. It involves the gravitational movement of sediments and water down a slope and causes a series of devastations along the path of travel. Often, it begins with a landslide and converts to flow depending on the hydrological conditions and gradient of the slope (Varnes, 1984). This phenomenon poses a serious threat to human life and the economic development of the affected region. The traffic corridor along the district road (M171) that connects Palani and Kodaikkanal is frequently affected by landslides, and several debris flows have occurred on this major district road that carries up to 2000 vehicles per day. Notable debris flow events occurred along the M171 in 2009 and 2014, while smaller occurrences are reported each year. In 2009, the incident led to road closure and severe disruption of traffic, while in the year 2014, enormous damage was caused in the plantations and heavy losses were reported. Despite these impacts, there was no loss of life or accounts of major injuries. Debris flows are less frequent than translational landslides in this region, but the impairment to infrastructure and loss of utility of roads caused by these disasters has a profound economic and social impact. These events have the potential to inflict serious injury to road users or can even lead to loss of life during periods of heavy tourist influx. Debris flows usually occur between October and November when there is prolonged and intense rainfall (monsoon), and the possibility of these episodes taking place during the intense summer showers between April and June should not be ruled out. There are currently no scientific records that describe the nature, source areas, volume, flow path, or deposition zones of debris flow incidences along the M171.

There are several methods such as empirical (Hungr et al., 1984; Rickenmann, 1999; Hürlimann et al., 2008), deterministic (Montgomery and Dietrich, 1994; Quan et al., 2011), probabilistic (Liang et al., 2012; Elkadiri et al., 2014; Lucà et al., 2014), and heuristic approaches (D'Ambrosio et al., 2006; Neaupane and Piantanakulchai, 2006; Sujatha and Sridhar, 2017) for the identification and mapping of debris flow susceptibility. The literature mentions that the most common factors used to assess debris flow are slope, grain size of soil matrix and soil type, hydraulic conductivity of soil, effective cumulative rainfall, effective rainfall intensity, watershed area, shape of watershed, length of creek, topography, geology, land use and land cover, discontinuities, and drainage pattern (Dai and Lee, 2002; Kondratyev et al., 2006; Hürlimann et al., 2008; Shieh et al., 2009; Quan et al., 2011; Liang et al.,

Received November 8, 2018; accepted May 17, 2019

E-mail: r.evangelin@gmail.com

2012; Okano et al., 2012; Elkadiri et al., 2014). The run-out distance, known as the area affected by the hazard, and energy along the flow path are also important for susceptibility mapping (Hürlimann et al., 2008). The dynamic method is most preferable for the determination of a debris flow hazard but is a very difficult task. Therefore, the assessment of debris flow hazards must rely on semiquantitative methods or numerical simulation models. Numerical simulations have restricted applications due to practical limitations such as being data intensive, and hence, can be applied only to discrete slopes or small areas (Rickenmann, 1999). They require soil strength properties including angle of internal friction, cohesion, pore pressure parameters, and unit weight that require extensive and elaborate sampling programs, and are therefore difficult to obtain.

Susceptibility maps depict the spatial disposition of areas prone to slope failure and do not yield information on the temporal occurrence of these events (van Westen et al., 2006; Keefer and Larsen, 2007; Fell et al. 2008). These maps can be prepared through either direct or indirect methods (Aleotti and Chowdhury, 1999; Guzzetti et al., 2006; Keefer and Larsen, 2007; Althuwaynee et al., 2015). The direct approach comprises extensive field surveys and studies for identifying and mapping the source areas of debris flow (Montgomery and Dietrich, 1994; Blahut et al., 2010; Quan Luna et al., 2011). This approach can be adopted when the study is limited to small areas or specific sites. The indirect approach involves susceptibility modeling using statistical, probabilistic, or heuristic methods (D'Ambrosio et al., 2006; Neaupane and Piantanakulchai, 2006; Liang et al., 2012; Okano et al., 2012; Elkadiri et al., 2014; Chen et al., 2017; Sujatha and Sridhar, 2017). These methods are based on the assumption that the occurrence of landslides or debris flows is a function of the geo-environmental conditions in the region and will also influence future incidents (i.e., future slope failures are based on historical events) (D'Ambrosio et al., 2006; Neaupane and Piantanakulchai, 2006; Blahut et al., 2010; Liang et al., 2012; Bregoli et al., 2015; Chen et al., 2017; Sujatha and Sridhar, 2017).

The lack of scientific evidence and a detailed inventory of debris flow events, their volume, and velocity restrict the use of statistical or probabilistic models for mapping susceptibility. Heuristic models based on expert knowledge can, however, bridge this gap of limited data availability or absence of official and scientific debris flow records. This study attempts to employ a less explored heuristic method, the analytical network process (ANP), to evaluate the spatial susceptibility of debris flow along the M171 highway corridor. The ANP was developed by Saaty (1980) and is a top-down decision model that is an extension of the analytic hierarch process (AHP). It is a multi-criteria decision tool that transforms subjective perceptiveness of relative importance to scores or weights. It is a unique mathematical theory that systematically deals with, and extends the analytical hierarchical process to, cases of feedback and dependencies and generalizes the super matrix approach (Saaty, 1980). The ANP is commonly applied in areas such as finance, economics, industrial management, forest management, highway planning, and construction planning and management (Sujatha and Sruthi, 2016). However, its applications in geo-engineering is very limited (Neaupane and Piantanakulchai, 2006; Sujatha and Sridhar, 2017).

This study is summarized as follows: an ANP model that considers the intradependence of the selected environmental factors was developed for mapping debris flow susceptibility. The factors causing debris flow were identified through extensive field surveys and inspections and include the nature of the slope forming material, hydraulic conductivity of geo-material and water conditions of the slope, slope angle, vegetation on slope, and drainage density. This model ranked and assessed the effect of the selected geo-environmental factors on debris flow susceptibility using scores termed as "priorities". These priorities were employed to assess the spatial susceptibility of the road sections to debris flow. Validation was carried out using the following two steps: (i) verification of debris flow susceptibility map using spatially partitioned validation data set of debris flow incidences and (ii) comparison with a deterministic infinite slope stability model modified to accommodate hydrologic parameters such as net rainfall and equilibrium soil saturation (Vanacker et al., 2003; Bregoli et al., 2015).

2 Study area

The highway corridor selected for this study stretches between Kumburvayal and Vadakaunchi, connecting Kodaikkanal, a popular hill station and Palani, a temple town (Fig. 1). Both destinations have a significant tourist influx all year round. The length of the road stretch is 5.51 km (77°32′27.6″E and 77°34′1.2″E longitudes and 10°17′31.2″N and 10°18′50.4″N latitudes) and is identified in the Survey of India topographic sheet No. 58 F11. This traffic corridor carries large volumes of traffic, particularly during holidays. Dissected slopes (73% of the area), a highly dissected plateau (27% of the area), and valleys are the prominent geomorphic features. The valley is evidenced as a narrow strip along the road following the northeast-southwest (NE-SW) trending fault. Croplands and plantations primarily cover the stretch, and there are also a few patches of barren land and forests.

The temperature is characteristic of the higher altitude of the region, and the average minimum and maximum are 5°C–12°C and 17°C–25°C, respectively. The region receives rainfall almost throughout the year, with maximum rainfall occurring in the northeast monsoon months of October and November. Records suggest that nearly 47% of the rainfall is received during this period.

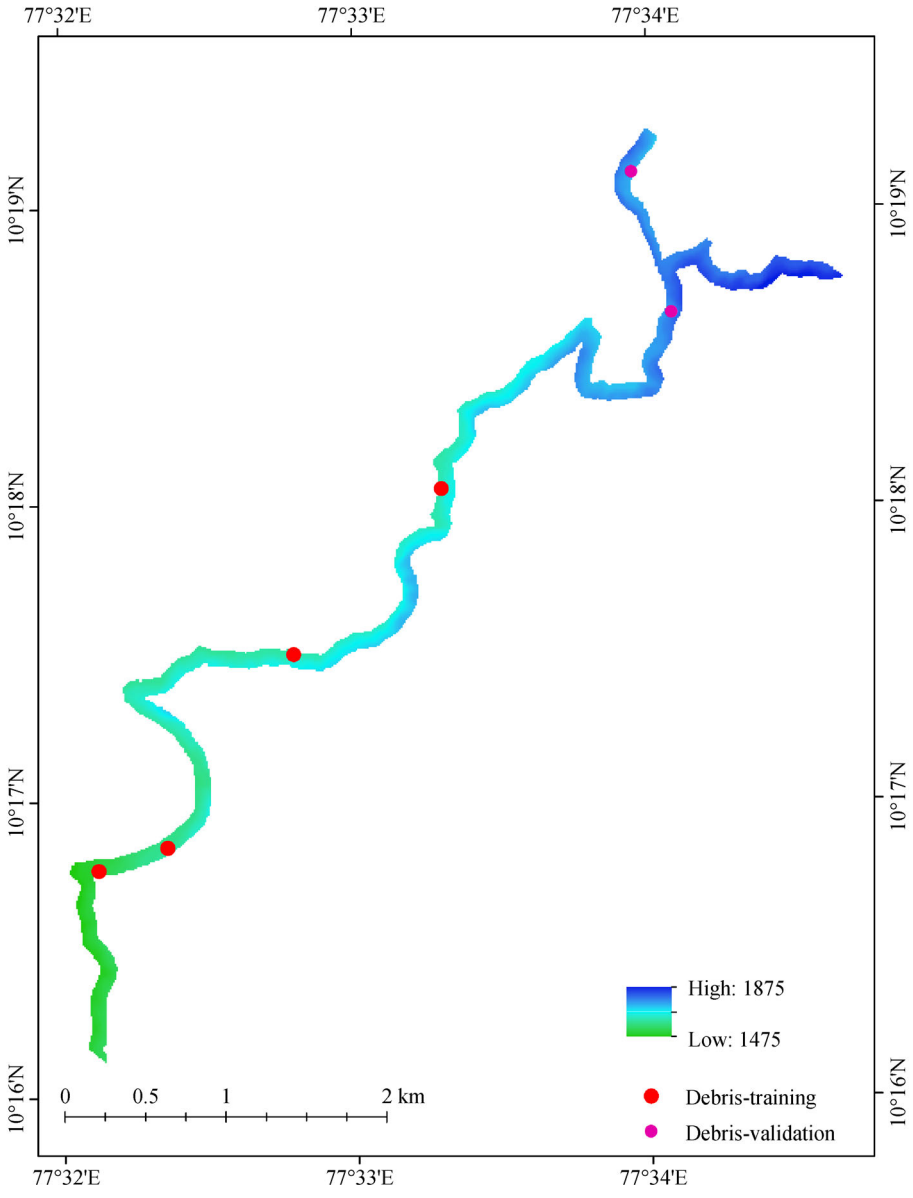

Fig. 1 Location map of the selected road stretch between Kodaikkanal and Palani (M171).

Minimum rainfall is received between mid-December and March, and the summer months of April and May also receive intense showers. The annual average rainfall varies between 1650 mm and 1800 mm. Fog is experienced during the winter months of December, January, and February, hail occurs in the summer months between March and May, and thunder is evident in both the summer and monsoon seasons.

3 Debris flow characterization

Debris flows are usually triggered by copious amounts of rainfall and are often characterized by the transformation of translational slides into flows that wash away the soil on the slopes while gathering momentum in the presence of water and moving down-slope as debris. Debris flows along the Kumburvayal-Vadakaunchi road stretch occur on the slopes covered with mostly granular, unconsolidated, superficial deposits and can be classified as open type (hill slope) (Cruden and Varnes, 1996). They form their path down the valley and deposit the debris scree or material on the lower slopes that have a less significant gradient. The debris material moved down the slope consists of loose deposits of gravel, small boulders, weathered and disintegrated rock, and coarse sand that are susceptible to the drag force exerted by water at moderate thrust and speed. The slopes in the region are relatively steep and their

heights range from 10 m to 15 m on average, augmenting the movement of material down the slope.

The slope forming materials move along the slope as debris flow and are deposited on the slopes further down as the flow loses its momentum by virtue of the load of the accumulated material, in addition to the reduced gradient further down the slope. The major debris flow events that occurred in 2009 and 2014 (Fig. 2) demonstrated that a substantial quantum of water was required to mobilize the debris. Slopes failed in locations where man-made water outlets cut across the slopes, aggravating the debris flow. The shallow roots of the plantations on the slopes including plum, peach, pear, banana, beans, turnips, and butter beans, etc. were not sufficient to arrest the movement of soil during the debris flow. Also, these plants and/or trees lost soil support during the movement and were washed along with the debris material. A large amount of debris was deposited down-slope along the valley, rendering the area uncultivable. To this day, the depositional area of the 2009 debris flow event still remains uncultivated and barren. The debris flow events are isolated and in the recent past, have not been reactivated in the same locations; however, adjacent stretches of the slopes are affected during subsequent rainfall.

4 Spatial database of factors causing debris flow

The study of the local geo-environmental and debris incidences along the selected road stretch and a comparison of debris flow events in a similar geo-environment bound by the same watershed boundary identified the following factors that cause debris flow in this region: (i) nature of the slope forming materials; (ii) hydraulic conductivity of the slope forming materials; (iii) slope angle; (iv) vegetation; and (v) drainage density.

4.1 Nature of slope forming materials

Debris flow mobilization depends on the gradation of slope forming materials (Gabet and Mudd, 2006), thickness of the material on the slope, and their degree of packing. Fine sand is more prone to complete loss of shear strength with an increase in pore pressure than clay rich soils owing to their lack of cohesion (McMillan et al., 2005). The potential for the occurrence of debris flow is much greater if the available material is granular with no cohesion and the particle size varies over a broad range (Sujatha and Sridhar, 2017). The geotechnical database developed for this study showed that the materials along the selected road stretch were granular in nature with very little or no cohesion. The particle size distribution of the debris material diverged over a very wide range from small-sized boulders (300 mm diameter), pebbles/cobbles, and coarse sand to fine sand. The major fraction (67%) of the deposit was sand with an effective size varying between 0.1 mm and 0.23 mm. The average uniformity co-efficient and co-efficient of curvature was 7.45 and 0.8, respectively. The percentage of fines was less than 5% in the representative

Fig. 2 Partial view of debris flow on a private plantation along the selected road stretch in 2014.

samples taken for analysis. The soil was classified as poorly graded sand according to the Unified Soil Classification System. The larger particles (pebbles/cobbles) were round to sub-round in shape, while particles in the gravel size were flaky. The majority of the larger particles were observed to be smooth, enabling easier mobilization of the material by water and causing debris flow.

The nature of the slope forming material depends on the thickness of the overburden (quantity of material), curvature of the slope on which the material rests, and lithology (quantity and quality). The limited variation in curvature and lithology along the selected road stretch makes the thickness of overburden the assessment criteria to evaluate the nature of the slope forming material. In this study, weights were awarded based on the thickness of the overburden. The thickness of the overburden along the entire stretch was mapped by field survey. Figure 3 presents the distribution of the thickness of overburden in the study area, which ranged from nearly bare to a maximum thickness of 8 m regolith on the slopes. The material was classified as shallow (<2 m), moderate (2–5 m), and thick deposits (>5 m).

4.2 Hydraulic conductivity

Debris flow is a water related hazard because water is required to mobilize the latent deposits on the hill slopes into debris flow. The rate of water infiltration, either as rainfall or overland flow, is vital for potentially mobilizing

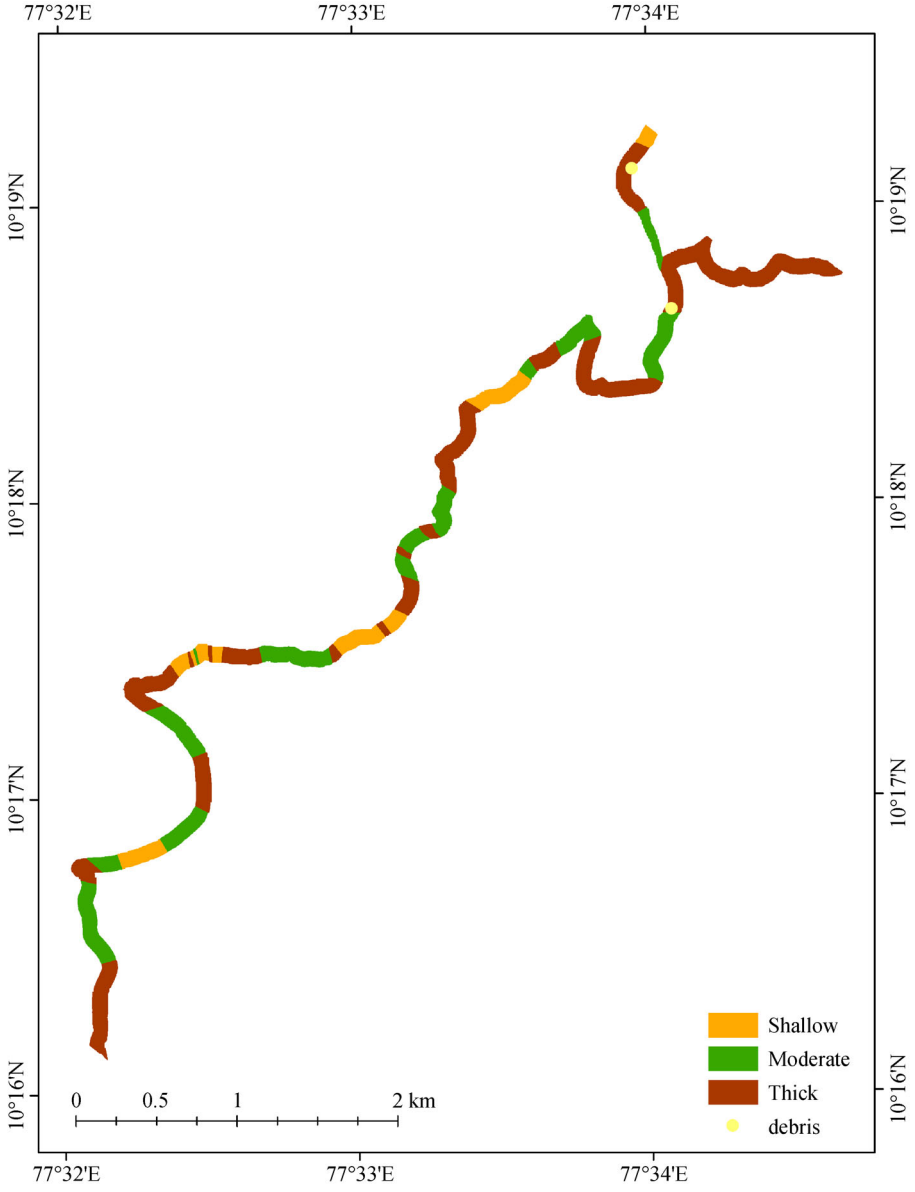

Fig. 3 Spatial variation of the availability of material to mobilize debris flow.

the deposits into a flow condition, and hydraulic conductivity plays a critical role in this process, particularly in weathered profiles (Santacana et al., 2003). Rocks were relatively impermeable along the selected road stretch with permeability in the range of 10^{-9} cm/s while the superficial material comprised of relatively clean gravel and sand characterized with a high permeability of 10 cm/s to 10^{-3} cm/s. Rocks existed as a continuum and did not form a part of the debris flow scree.

However, in certain sections along the road stretch, the rocks were weathered with a fractured and jointed rock fabric, and in these zones, the joints and original foliation formed cuboidal blocks out of the rocks that were susceptible to movement. The superficial deposits found in the region were a mixture of coarse sand and gravel, coarse sand, and fine sand. Hydraulic conductivity was determined from the constant and falling head permeability tests performed on the soil samples collected from the site. The tests were carried out as per IS: 2720-2006 standards. Hydraulic conductivity, being a function of effective particle diameter, varied with the gradation of soil and ranged between 10 cm/s for the coarse sand and gravel mixture to 4×10^{-3} cm/s for fine sand. The hydraulic conductivity was classified into low, moderate, and high categories, and Fig. 4 shows the spatial distribution of these classes.

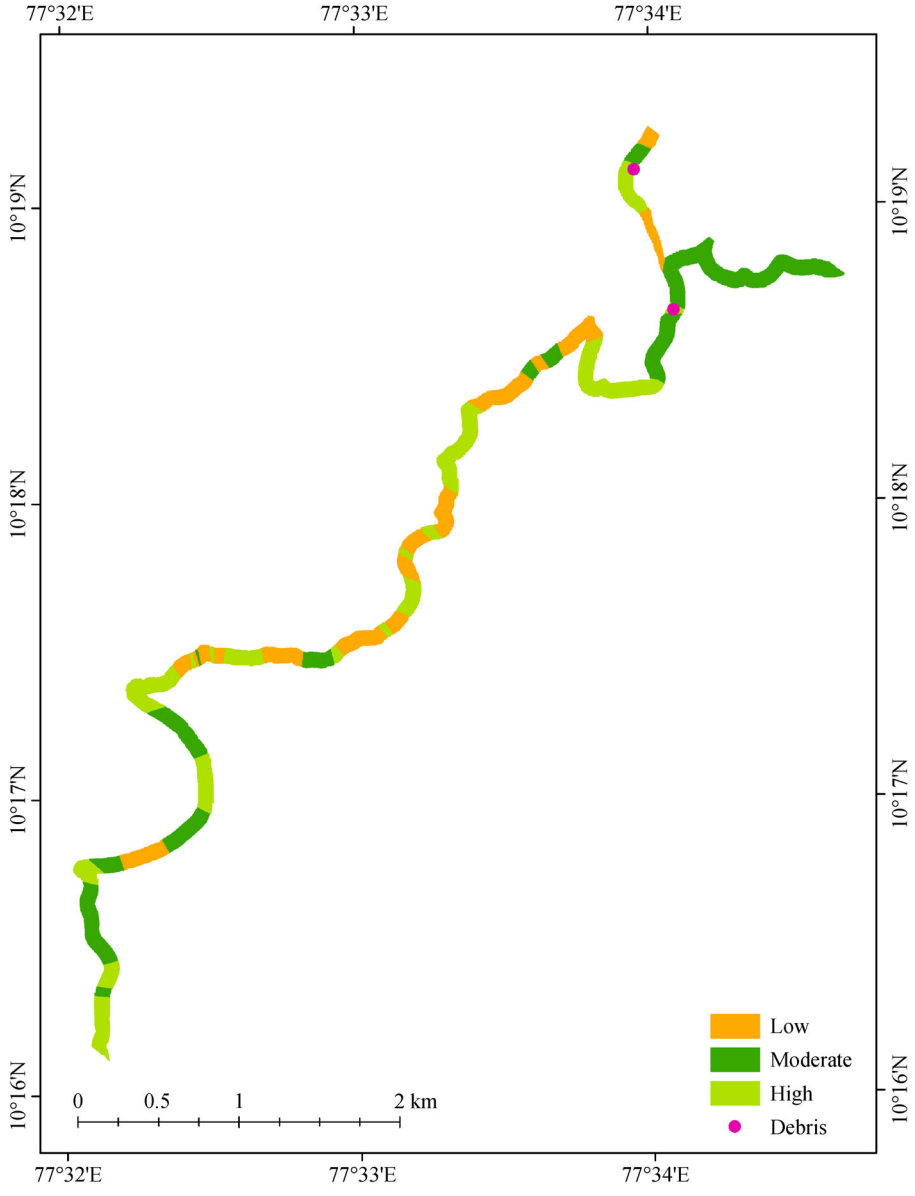

Fig. 4 Spatial distribution of overburden hydraulic conductivity.

4.3 Slope angle

The slope angle influences the susceptibility of a slope to debris flow, which increases with slope angle, but is limited by the steepness of the slope that prevents soil development and accumulation of debris material (Elkadiri et al., 2014). The slope influences the supply of debris material, size of the debris flow, and its volume (Chen et al., 2017). The slope map in Fig. 5 was generated from the contour map (derived from the 58F11 topographic sheet) with 10 m contour intervals using the spatial analyst tool in ArcMap 10.2. The natural slope angle ranged from 1.27° to 61.25° and the mean of slope angle distribution was 27.21°. The road cuts were steeper and made to near 80°.

Natural slope angles are used for mapping debris flow susceptibility as cut-slope angles are discrete and show abrupt changes that do not characterize the nature of the terrain. The slope angles were classified into gentle (0°–15°), moderate (15°–35°), and steep ($>35°$) categories. As shown in Fig. 5, it was observed that the majority of the slopes along the selected stretch fell within the 15°–35° slope angle range.

4.4 Vegetation cover

Vegetative cover on slopes affects slope stability, particu-

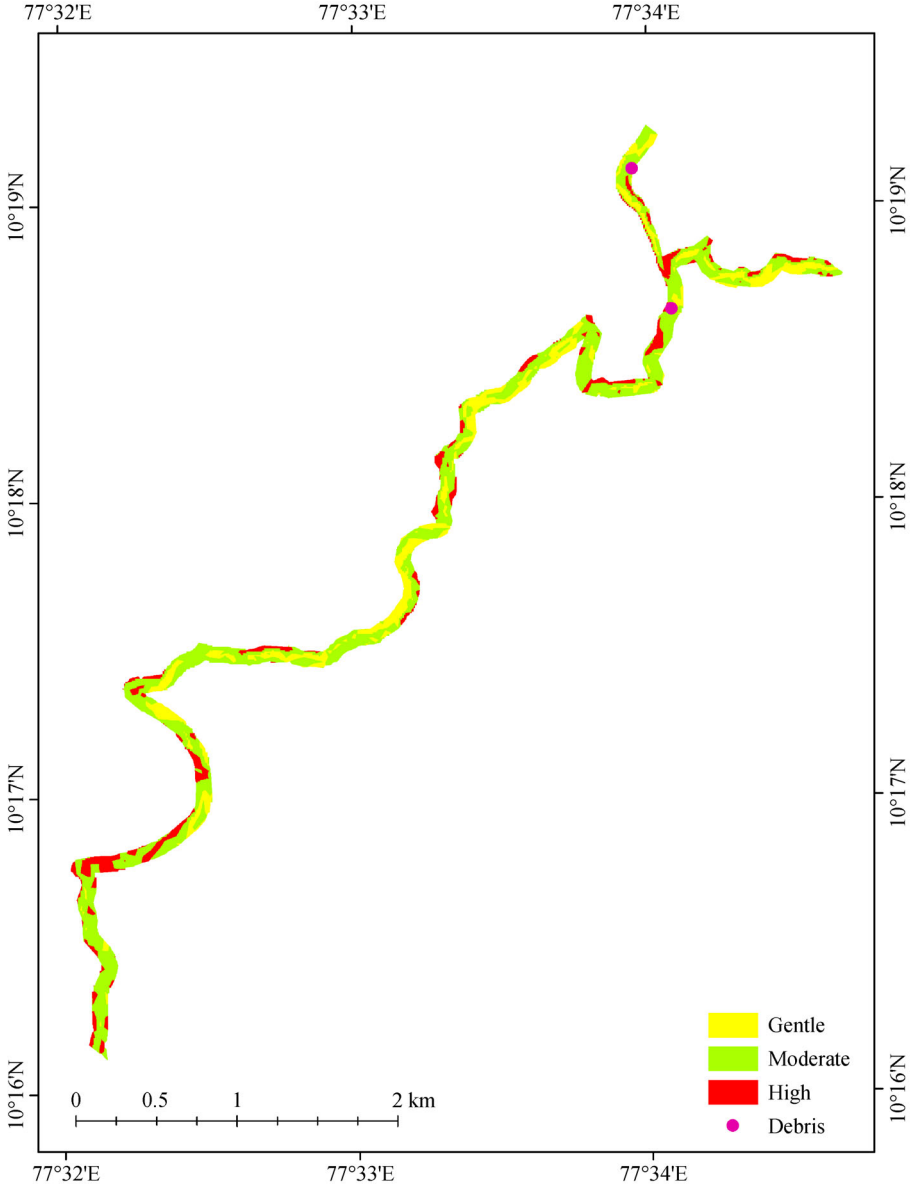

Fig. 5 Spatial variation of slope along the selected stretch.

larly in the case of shallow landslides. Trees with strong root systems are effective at holding the soil and preventing their movement (Franks, 1999; Sujatha and Sridhar, 2017). The land use map (Fig. 6) of the study area was derived from the World View 2 satellite data at 2.5 m resolution (Date of Pass: January 5, 2013).

A thorough field verification was completed in order to refine the land use categories for a detailed analysis. Croplands, plantations, open scrubs, and wastelands covered the slopes in this region. For this study, the land use and land cover system were reclassified into forests, plantations (inclusive of croplands and plantations), and barren land (inclusive of rocky wastelands and open scrubs) (Fig. 6).

4.5 Drainage density

Debris flow events are closely associated with streams and stream paths that act as conduits for the movement of debris (Fig. 7) and are also a chief source of water that aids in dislodging and moving the material down the slope. Numerous first order streams that cut through the slopes augment erosion, and when the flow of water is moderate, debris material is deposited on stream beds and form debris dams (Winter, 2013).

The stream network derived from the topographic map

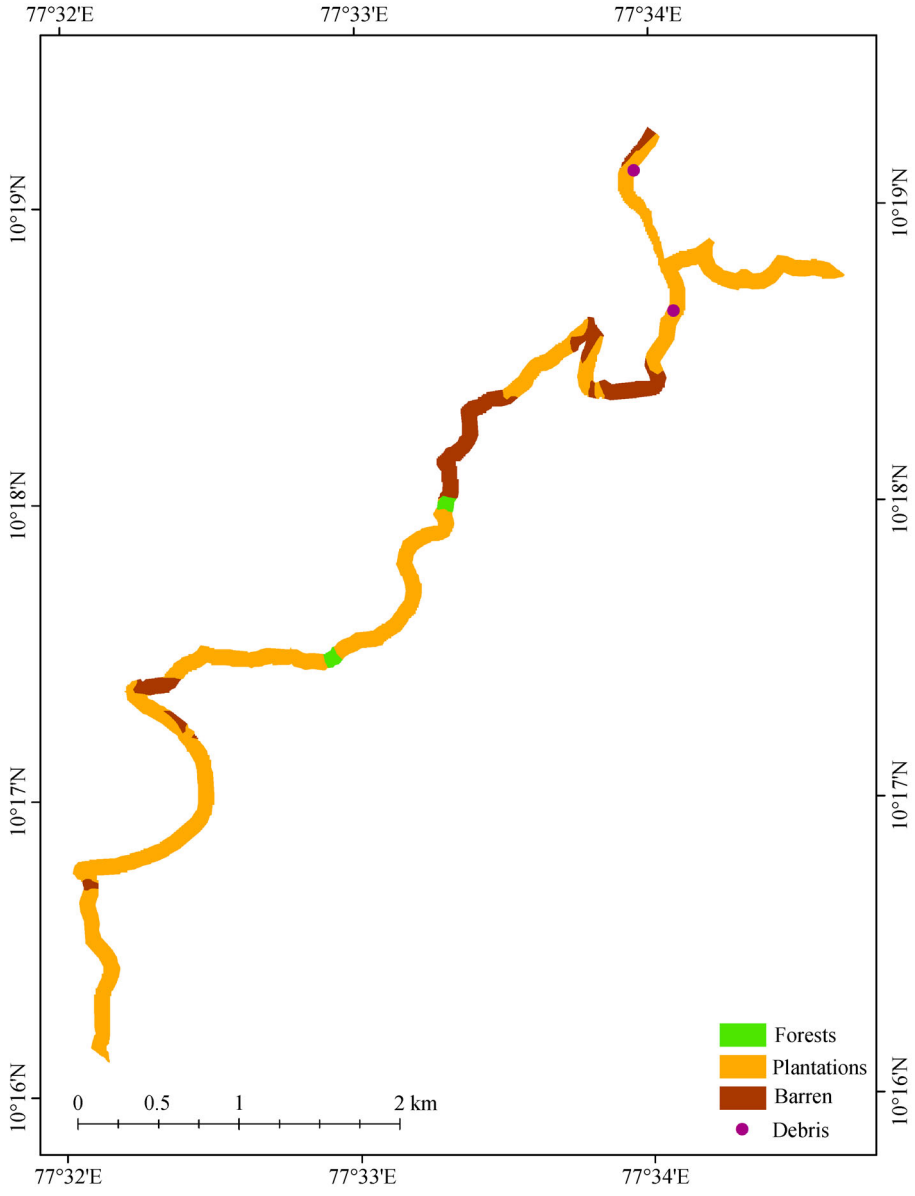

Fig. 6 Land use and land cover distribution.

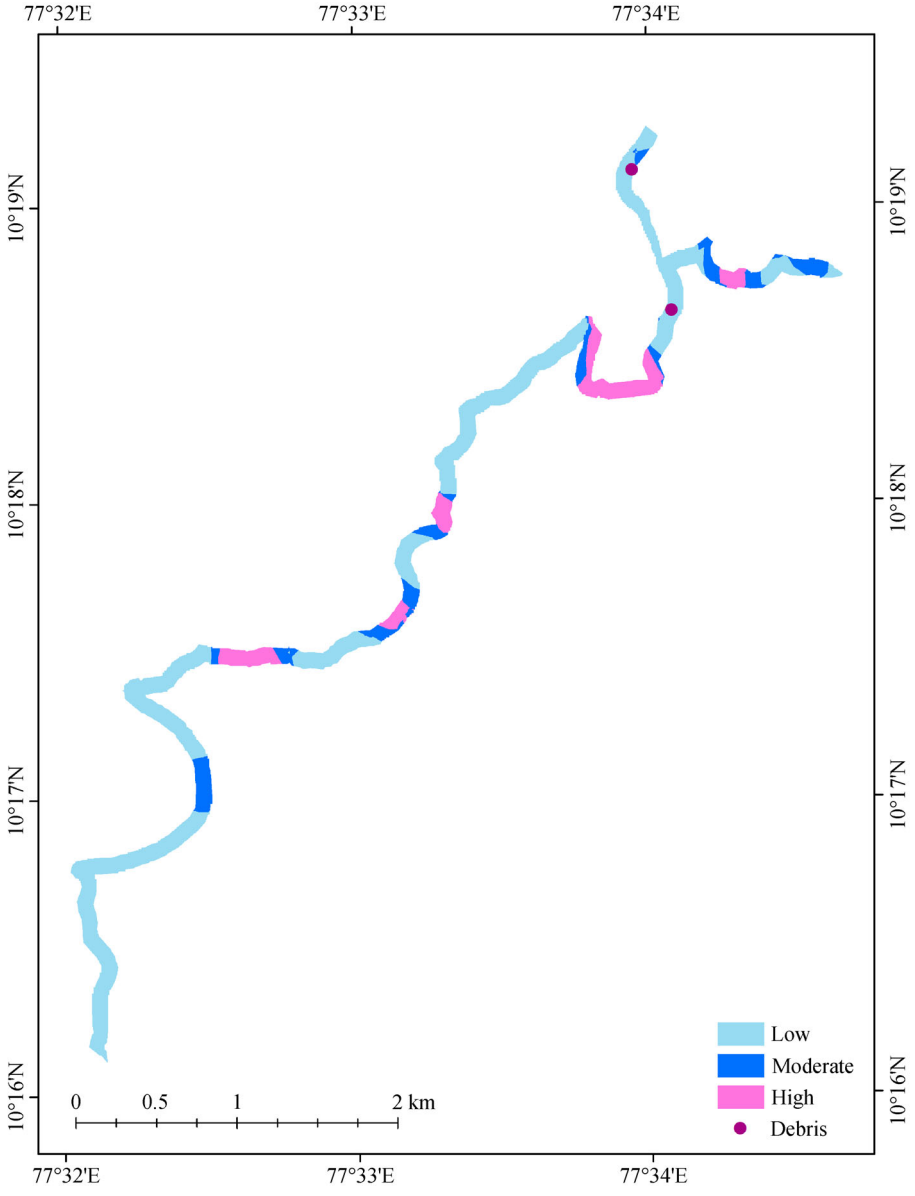

Fig. 7 Spatial variation of drainage density.

58F11 shows that there are numerous first order streams in the study area. As a consequence of several lower order streams, a large number of stream confluences are present, which according to Lee et al. (2003), can be attributed to the heterogeneity of channel morphology. These stream confluences are prone to debris flow. Drainage density, which indicates the stream length per square unit area, is used to measure the influence of the presence of streams. The drainage density map was derived from the stream network using focal statistics of the spatial analyst tool in ArcMap 10.2. The drainage density varied from 1 km/km^2 to 410 km/km^2 and was reclassified using natural breaks into low, moderate, and high categories (Fig. 7).

5 Debris flow model using the Analytical Network Process (ANP)

In the absence of scientific records of the debris occurrences in the study area, debris flow locations were identified via intensive field surveys along the selected road stretch. Local knowledge of the residents on these events was also taken into consideration to verify the authenticity of the locations. As previously mentioned, more debris flow incidences are reported by residents of the area, but it was only possible to identify six locations in the field. This limited the options available to this study to less data intensive models for assessing the susceptibility

of debris flow in the region, and therefore, a model with the heuristic approach that can incorporate expert knowledge was more suitable. Hence, a decision model, the ANP, was used to assess the contribution of different geo-environmental factors in mapping debris flow susceptibility. The limited available data set was divided spatially into training and validation data sets. The study area, an 8 km road stretch along the M171, was split into training and validation segments. The longer stretch, 6 km with four debris flow locations to the south, was used to identify the factors causing debris flow and to develop the pairwise comparison matrices while the remaining 2 km of road with two debris flow events, was used to validate the debris flow susceptibility map generated from the ANP model. Another advantage of using the ANP is its ability to allow for interdependencies. Some geo-environmental factors that cause debris flow are not mutually independent but are influenced by other factors. This component of interdependency between selected parameters can be effectively modeled using the ANP.

The Analytical Network Process is a multi-criteria analysis tool that models interdependent relationships i.e., hierarchically non-structured relationships with interaction and dependencies (Saaty, 1980; Sujatha and Sruthi, 2016; Sujatha and Sridhar, 2017). An ANP model comprises three fundamental clusters including goal, criteria, and alternatives and consists of the following four phases:

1) Structuring the decision network where the network model is built based on the objective and is split into clusters comprising of nodes (elements) and alternatives (Fig. 8). The relationship between nodes within and outside the clusters are identified. Each element in the cluster can either be a source (i.e., an origin in the path of influence) or a sink (i.e., destination in the path of influence) (Neaupane and Piantanakulchai, 2006).

2) A pairwise comparison where judgments rely on rating factors in comparison with each other based on the fundamental analytical hierarchical process scale and arranging them in a pairwise comparison matrix. The priorities or the weights are obtained by solving for the principal eigenvector of the matrix. These matrices have more than one eigenvector; the principal eigenvector, which is associated with the principal eigenvalue λ_{max} (i.e., the largest eigenvalue) of the pairwise matrix, is the solution vector used for an AHP pairwise comparison matrix (Saaty, 1980)

3) Construction of the super matrix to assess the priorities that exist between the elements (Saaty, 1980). The unweighted super matrix consists of several eigenvectors, the sum of which is one (Neaupane and Piantanakulchai, 2006), and contains the local priority vectors of the comparison groups in the network. Elements of the interdependent network range between zero and one and zero for an independent network. This matrix is converted to a weighted super matrix in which the sum of the individual columns is unity and is obtained as the product of the node in the cluster and weight of the cluster (Saaty, 1980). It is raised to powers till it converges to all columns in the super matrix having the same value and this iteration is then called the limiting super matrix. It consists of the priorities or weights of the alternatives as well as the

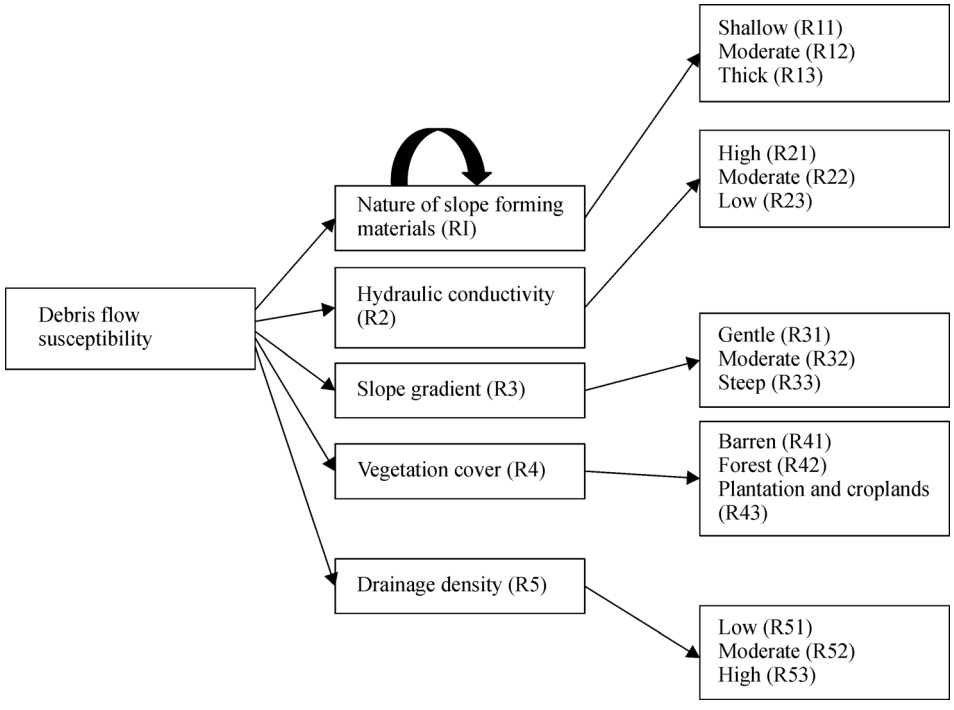

Fig. 8 Debris flow susceptibility decision frame in the ANP.

other elements in the model.

4) Global priorities (i.e., weights) are also calculated from the super matrix (Saaty, 1980). These weights are then awarded to the thematic layers and the sum of the weights in each unit polygon gives the debris flow susceptibility. The ANP model was developed using the Super Decisions software.

Figure 8 shows the ANP model used to assess the debris flow susceptibility, and the cluster criteria consisted of the following nodes: nature of slope forming material (R1), hydraulic conductivity (R2), slope angle (R3), vegetation (R4), and drainage density (R5). Node R1 was dependent on R2 and R3 while the node R4 depended on R1 and R2. This made the cluster criteria intradependent with a self-loop. The cluster alternatives consisted of the subcategories of the factors (nodes) in the criteria cluster. Each node in the criteria cluster was connected to its relevant subcategories in the alternatives cluster. For example, the node nature of slope forming material in the cluster criteria was connected to the nodes R11 (shallow thickness of overburden), R12 (moderate thickness of overburden), and R13 (thick overburden) in the alternative cluster. The pairwise comparison matrices (Fig. 9) were developed based on the training data set. The pairwise comparison matrix rated each factor with respect to the other on a scale of 1–9 (Saaty, 1980), and an example is shown in Fig. 9. The super matrix was created from the comparison matrices, which in turn, was employed to assess the priorities of the factors selected for modeling debris flow. The priorities were based on the interdependencies of the factor, and these priorities were used as weights to model debris flow susceptibility.

The maximum priority or weight was awarded to low permeability and the minimum to forests (Table 1), meaning that low permeable material were most susceptible to debris flow while forests deterred the mobilization of debris flow to a great extent. Low permeable material were more susceptible to failure due to high pore pressure buildup, and therefore, a higher reduction in shear strength as a result of greater pore pressure. Priorities or the ranking of the selected parameters are shown in Table 2.

6 Debris susceptibility map and validation

The thematic layer of each factor identified to cause debris flow was awarded a weight based on the scores/global priorities obtained from the ANP model for each category of the thematic layer (Table 1). The thematic layers were then added using the union function of the analysis tool in the ArcMap 10.2 environment. The sum of the global priorities or weights yielded the degree of susceptibility to debris flow (i.e., the algebraic sum of the weights of the factors was used to measure the debris flow susceptibility (DFS)),

$$\mathrm{DFS} = \Sigma\text{Global Prioties (or) Weights.} \quad (1)$$

The descriptive statistics of the spatial distribution of debris flow susceptibility showed a minimum, maximum, mean, and standard deviation of 0.0374, 0.64135, 0.3795 and 0.1428 respectively. As shown in Fig. 10, the resulting debris flow susceptibility map was reclassified into three classes of low, moderate, and high. Approximately 23% of the road stretch was highly susceptible to debris flow and 40.5% fell under the low susceptible category.

The debris flow susceptibility map constructed from the ANP model was validated through field inspections of susceptible sites and comparison of debris flow events from the validation data set. Both the debris flow locations in the validation site fell within the high susceptible zones of the generated susceptibility map. This indicates a 100% success rate for the ANP debris flow model; however, this success rate should be viewed with caution as the data set is extremely limited.

Extensive field investigations were carried out to ascertain the correlation between the geo-environmental

Fig. 9 A pairwise comparison matrix for the cluster criteria.

Table 1 Weights of alternatives for modeling debris flow susceptibility

Alternatives	Priorities/weights	Alternatives	Priorities/weights
Shallow thickness of overburden (R11)	0.05580	Barren land/open scrub (R41)	0.08162
Moderate thickness of overburden (R12)	0.17715	Plantation and cropland (R42)	0.02295
Thick overburden (R13)	0.14061	Forests (R43)	0.00645
Low hydraulic conductivity (R21)	0.21082	High drainage density (R51)	0.00235
Moderate hydraulic conductivity (R22)	0.05502	Moderate drainage density (R52)	0.02973
High hydraulic conductivity (R23)	0.01795	Low drainage density (R53)	0.05502
Gentle slope (R31)	0.01209		
Moderate slope (R33)	0.14203		
Steep slope (R32)	0.03707		

factors and debris flow susceptibility in the validation site, as well as the success of the resulting debris flow susceptibility map.

Additionally, the resulting debris flow map was compared to a deterministic infinite slope stability model that was combined with a steady-state hydrologic model (Vanacker et al., 2003, Bregoli et al., 2015). This is a process-based model and is used to predict the spatial distribution of slope movement. The conventional infinite slope stability model based on the limit equilibrium method was modified to accommodate the effect of vegetation, degree of soil saturation, and thickness of the soil cover. The model uses the Mohr-Coulomb failure criteria and the factor safety, which denotes the susceptibility to debris flow. The hydrologic model maps the spatial distribution of the equilibrium soil saturation based on the local slope, upslope contributing area, and transmissivity (Montgomery and Dietrich, 1994; Vanacker et al., 2003; Bregoli et al., 2015). The factor of safety is computed as:

$$\text{Factor of safety (FOS)} = \frac{c + c_r + (\gamma - \gamma_w m) z \cos^2\alpha}{\gamma z \sin\alpha \cos\alpha} \tan\varphi', \quad (2)$$

where c is the cohesion of the soil (kPa), c_r is the root cohesion (kPa), a component that describes the effect of vegetation on the slopes, γ is the unit weight of the soil (kN/m^3), γ_w is the unit weight of water (kN/m^3) that accounts for the pore water pressure, z is the soil thickness (m), α represents the local slope (°), φ' is the effective angle of internal friction (°), and m is the soil saturation. This model can be applied only to soil slopes, and hence, parts of the road stretch with no soil overburden (i.e., rock slopes were ignored in the analysis).

The equilibrium soil saturaion is represented as a function of the factors described in the equation below:

$$m = \frac{qa}{bT\sin\alpha}, \quad (3)$$

where q is the net rainfall (m/s), which represents the infiltration of rain water into the soil and is the difference between the rainfall rate and sum of potential evapotranspiration and rainfall interception (%); a is the upslope contributing area; b is the width of the slope, which is taken as the pixel resolution (m); and T is the transmissivity, the product of permeability of the soil (m/s) and soil thickness (m).

Table 3 presents the model input parameters used for the geotechnical model that depends on the land use category. The parameters such as cohesion, angle of internal friction, and unit weight of the soil were determined through laboratory investigation on the soil samples collected from the field along the selected road stretch. Soil along the slopes on the selected road stretch, as observed from the visible road cuts, was usually in two layers: a very thin top soil cover, which was dark gray to black in color, followed by red gravelly sand. The thin layer of the top soil ranged from 10 cm in thickness to a maximum of 50 cm and was rich in organic content with a pungent odor. The red soil below ranged in thickness from 1 m to a maximum of 15 m. Soil samples were collected at 16 locations for determining the engineering properties of the soil. Cohesion varied between 0 kPa and 22.5 kPa, the angle of internal friction from 0° to 43°, and unit weight from 0 kN/m^3 to 19.3 kN/m^3. The soil thickness was determined

Table 2 Priorities of the nodes in the criteria cluster (factors causing debris flow)

Factors	Weights/priorities	Factors	Weights/priorities
Nature of slope forming material (R1)	0.37356	Vegetation (R4)	0.11103
Hydraulic conductivity (R2)	0.28379	Drainage Density (R5)	0.04044
Slope (R3)	0.19119		

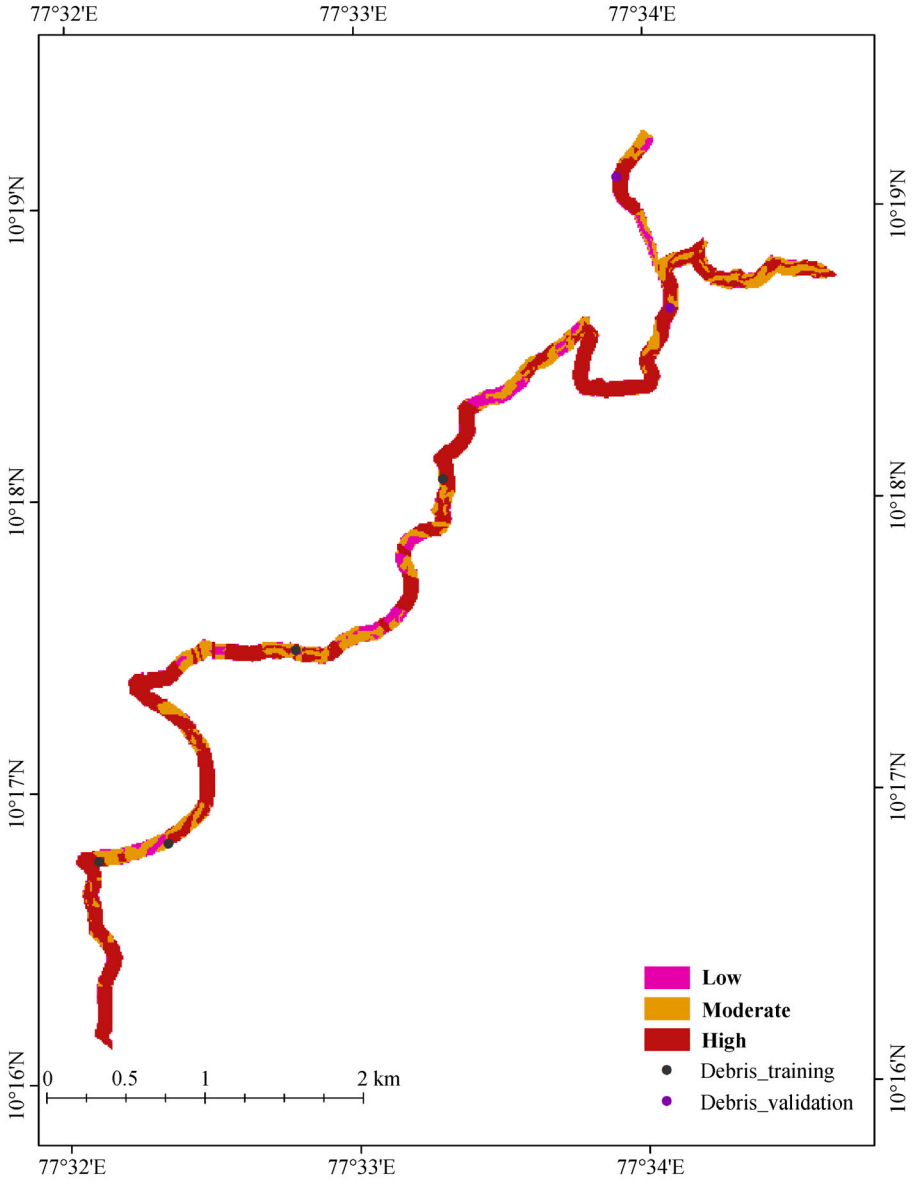

Fig. 10 Debris flow susceptibility map of the selected road stretch using an ANP model.

Table 3 Input parameters for the infinite slope stability model based on land use

Factor	Unit	Barren/open scrub	Plantation/cropland	Forest
Root cohesion (c_r)	kN/m^2	0	0	12
Total rainfall (Q)	m/s	9.92E-07	9.91E-07	9.9E-07
Evaporation (E_v)	m/s	6.94E-08	3.47E-08	0
Rainfall interception (R_i)	%	0	11	30
Net rainfall	m/s	9.22E-07	8.48E-07	6.9E-07

by extensive field surveys and mapping, and the slope was extracted from the Advanced Spaceborne Thermal Emission and Reflection Radiometer (ASTER) Global Digital Elevation Map (DEM) (30 m × 30 m) of the study area. Massive rock slopes with no soil cover were neglected. The raster layers of the factors were combined to produce the factor of safety map, and the factor of safety ranged between 0.4 and 8. Slopes with a factor safety below 1.5

were classified as highly susceptible to debris flow and those above 4 as least susceptible. The resulting factor of safety map (Fig. 11) that represents debris flow susceptibility, closely matched with the debris flow susceptibility map derived from the ANP model, particularly where debris flow incidences occurred. These findings prove that the ANP can be successfully used to map debris flow susceptibility.

7 Discussion

This study demonstrates that the analytical network process (ANP) is effective at modeling debris flow susceptibility, particularly in cases where limited data are available. It provides a greater scope for expert judgment and allows for interdependencies between the factors that cause debris flow. Most statistical models such as generalized linear regression, logistic regression, weights of evidence, and certainty factor, etc. do not allow for interdependencies between the factors (i.e., each factor tends to behave like an independent factor), but the ANP allows for interdependency between any two factors, which reflects the field conditions more appropriately. This is one of the significant advantages of this model, as it allows the user to model the influence of one factor on another if an interdependency exists between them. The model ranked the factors considered in this study according to their influence in initiating debris flow. The nature of the slope forming material rated as the most

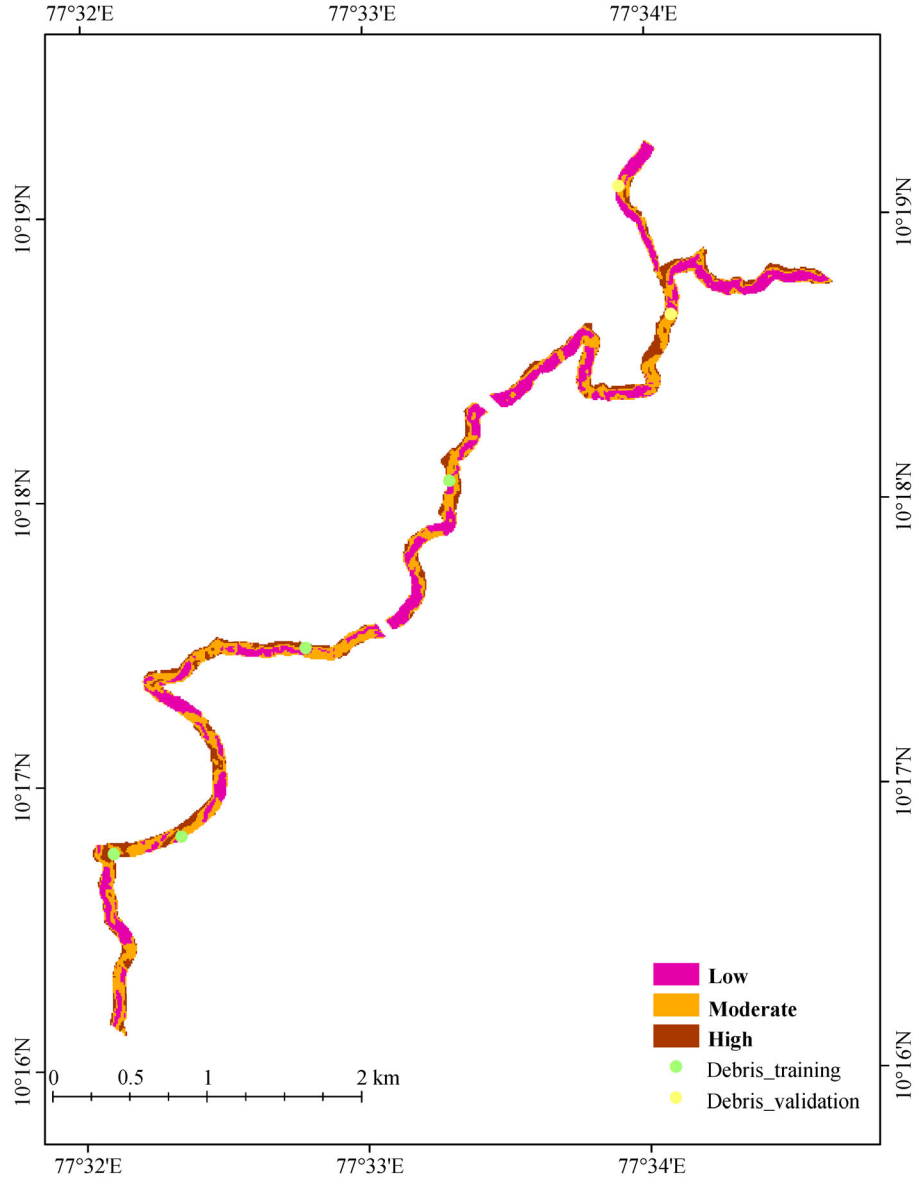

Fig. 11 Factor of safety map based on a deterministic infinite slope stability model combined with a steady-state hydrologic model.

important factor causing debris flow along the selected road stretch, followed by the hydraulic conductivity of the soil, while drainage density was found to have the least effect in causing debris flow. The slope gradient and vegetative cover on slopes had nearly equal weights (Table 2).

The severity of debris flows depends on the magnitude and velocity of flow, and the nature of the slope forming material dictates the volume of material available for the event (i.e., it controls the magnitude of a debris flow event). The greater the quantity of loose, unconsolidated material on the slope, the greater the magnitude of the debris flow. The soil/overburden cover in this region is predominantly sandy in nature with little or no cohesion. The soil is characterized by low unit weight and granular nature. The lack of cohesion in the fines content of the soil over the slope provides a greater impetus for the mobilization of debris flow, as these deposits lack the binding force to be held together and are more prone to erosion, particularly when rainfall is intense and continues for long periods of time (Sujatha and Sridhar, 2017). Though the granular soil has considerable shear strength owing to higher angle of internal friction, during intense precipitation, effective stress reduces drastically due to an increase in pore pressure. This causes the rapid loss of strength, and furthermore, the permeability of the soil on the slopes differ exponentially from that of the bedrock. The soil/overburden material on the slopes in this region was well-drained to moderately drained with permeability in the range of 10 cm/s to 10^{-3} cm/s, while bedrock was almost impermeable with permeability less than 10^{-9} cm/s. A restraint imposed on the movement of water at the interface of the soil and bedrock causes a substantial increase in the pore pressure at the contact surface. The change in direction of water due to the difference in permeability and the loss of shear strength at the interface leads to down-slope movement of the material on the slopes, particularly when the soil thickness on the slopes is limited to 5 m as was observed from field inspections. With respect to thick soil slopes, an increase in pore pressure causes the slopes to fail and this material is washed away as debris flow. The quantum of material washed away due to debris flow is greater when the thickness of the overburden on the slopes is greater. When a large quantity of overburden material is removed from a slope, the momentum of this flowing material causes further damage en route further down the slope. Hence, the thicker the overburden, the greater the susceptibility to debris flow.

The hydraulic conductivity of the slope forming material controls the rate of movement of water through the soil matrix, and hence, is a very important factor in mobilizing the materials for a debris flow event. The soil along the road stretch in the study varied from a coarse sand gravel mixture with very high hydraulic conductivity (10 cm/s), to fine sand with moderate hydraulic conductivity (10^{-3} cm/s). A higher rate of hydraulic conductivity indicates a high rate of infiltration into the soil. It allows for free drainage and less or no pore pressure buildup in the soil, and hence, is a preferred scenario when there is no excess water due to intense precipitation or flooding. However, during these extreme events, the effective stress is reduced and reaches shear failure due to the increase in pore pressure. The sustained and rapid supply of water into these soils promotes a transformation of the loosened slope material into a swift flow (Iverson, 2005; Iverson et al., 2010). Slope material is classified in terms of its hydraulic conductivity, and lower hydraulic conductivity indicates higher pore pressure buildup and greater chances of debris flow initiation . In this context, fine sand is more susceptible to debris flow than the coarse sand gravel mixture. Also, water present in the deposits leads to the buildup of pore pressure depending on the hydraulic conductivity of the soil, causing a destabilizing force that significantly reduces the shear strength of the slope forming soil, thereby resulting in failure. Studies reveal that slope normal infiltration is much higher than slope parallel drainage on fairly homogenous deposits (Iverson, 2000), as was the case in the region under study. When the bedrock below the mobile debris deposits is impermeable, the slope normal infiltration is impeded at the interface between the superficial deposit and the substrate (Winter, 2013), which again was the case here. This leads to the buildup of pore pressure and an increase in slope-parallel seepage forces, which initiates debris flow. The bedrock material in the selected study area was impermeable with respect to the high intensity rainfall event in most places. But in places where the bedrock was permeable, the slope normal hydraulic conductivity was higher, causing a reduction in the pore pressure, which thereby increased the shear strength and reduced the susceptibility to a debris flow event. Another major impetus to debris flow came from the pre-existing drainage system and water outlets that exhaust the rain water collected from the roads. This significantly affects the pore-pressure distribution in the superficial material and determines the passage, infiltration, and ponding of water (Winter, 2013). It was observed that in the 2014 debris flow event in Kumburvayal (Fig. 3), the water outlet draining the water from the upper reaches of the slope played a vital role in mobilizing the superficial deposits into debris flow.

The slope gradient is often one of the most important factors that causes shallow slope failures (Iverson, 2000; Keefer and Larsen, 2007; Elkadiri et al., 2014; Lucà et al., 2014, Sujatha and Sridhar, 2017). Slopes with a steep gradient have a greater potential to fail, but when the slopes are steeper, the loose unconsolidated material on the slopes move downwards due to gravity. Field surveys determined that on slopes greater than 35° the thickness of the overburden is usually limited. Steep slopes are also suggestive of material that possess good shear strength (Winter, 2013). Hence, slopes that have a slope angle greater than 35° are not usually susceptible to debris flow.

Similarly, when the slope gradient is less than 15°, the slopes are not susceptible to failure by virtue of their gentle gradient. However, when the slope gradient ranges between 15° and 35°, the thickness of the slope material is usually higher than that of the steeper slopes and the slopes are more susceptible to failure than the gentle slopes. Furthermore, the presence of vegetative cover and the nature of the slope material (type of soil, unit weight, thickness of overburden, and permeability) on these slopes augment their tendency to fail. Field observations and historical debris flow events also reinforce this fact. In this study region, it was observed that debris flow occurred frequently on slopes of gradient between 25° and 35°. It was also established that the slope gradient was not an independent factor that causes debris flow but was dependent on the nature of the material and the vegetative cover. The slope steepness provides the impetus for material to move down-slope and this is controlled by the tendency of the material to be dislodged from the continuum and also can be deterred by the presence of vegetative cover on these slopes.

Land use and land cover of a slope play a vital role in controlling the magnitude and velocity of a debris flow event. The presence of vegetation on the slope impedes the slope material against down-slope movement as the roots act like reinforcements and hold the soil that tends to move downward. This action of the roots also reduces the susceptibility of the soil to erosion and is particularly true in the case of shallow mass movements. The slopes in the study area were more granular in nature and the presence of vegetation played a vital role in preventing the soil matrix from erosion as the soil lacked cohesion. The vegetative cover on the slopes acts as physical barrier for the downward movement of the material (Neaupane and Piantanakulchai, 2006). The presence of vegetation also controls the moisture movement in the slope material and alters the evapotranspiration regime. The study area was predominantly covered by plantations and croplands, and barren stretches were also present with small patches of forest. Barren slopes with thick overburden are more susceptible to debris flow, while slopes covered with plants of wide root networks increase the stability of the slope material against movement. Slopes with croplands and plantations are also susceptible to debris flow because their shallow roots and also irrigation systems to water the plantations and orchards increase the moisture content on the slope (Sujatha and Sridhar, 2017). Forested areas are most stable against debris flow owing to their thick canopy and widespread root networks.

The drainage density reflects the fluvial dissection of the terrain and is an indirect measure of ground water conditions. In addition, it reflects the hydrogeological nature of the terrain. The stream path often acts as channels for the mobilization of the debris material down-slope. The region has many single order streams of small lengths which can be crucial in maintaining the momentum of the debris flow along the slope. A higher rate of percolation of rainwater occurs in areas of low drainage density, making these areas more susceptible to failure, which means that the lower the drainage density, the higher the rate of percolation. The unsaturated soil generates transient flow conditions in the soil matrix, and this effect is accentuated by the presence of deposits with high to moderate permeability. The presence of assorted particles of gravel size and above (>4.75 mm) also cause turbulent flow with the rapid ingress of water, particularly during heavy and continued rainfall. In line with this, all debris flow incidences, both in the training and validation data set, fell in the low drainage density category. The study area was characterized by long stretches of low drainage density, implying that the selected region is susceptible to debris flow.

The debris flow susceptibility map indicates that nearly 23% of the road stretch fell under the high susceptibility category. These sections of the roads are prone to closure during periods of intense and continuous rainfall. The thickness of slope forming material and its hydraulic conductivity are the key contributors to debris flow. However, slope modification, choice of the right type of vegetative cover, and proper drainage can help to stabilize these slopes against debris flow. Shola grasses can be planted in these sections to hold the loose soil in an effort to control the material available for initiation of debris flow. Similarly, hedge cultivation and turfing the cut slope with these grass varieties can regulate the ingress of water into the soil, which can also help in reducing the chances of the occurrence of debris flow. Shola grasses are especially preferred in these regions because they are endemic and have been lost due to introduction of eucalyptus plantations and their root systems can bind soil in the top 2–3 m, thereby proving very effective in controlling debris flow.

8 Conclusions

The ANP model has successfully identified the factors that cause debris flow and ranked them according to their importance in causing the events. This model has shown that it can be a useful tool in areas of insufficient data. The study reveals that:

1) Slopes made of thick deposits of granular material with low permeability are susceptible to failure as result of high development of pore pressure and drastic reduction in shear strength due to intense precipitation. This happens in a physical setting where the slopes are neither too gentle nor steep.

2) Another important component is the absence of vegetation with a strong root system, which includes plantations with shallow roots and a large of expanse of land in-between the plantations that are void of any vegetative cover.

3) Additionally, the irrigation provided for the plantation

also increases the wetness of the slopes, and further, it increases the weight of the overburden due to saturation while decreasing the shear strength of the soil.

4) Lower drainage density is another factor that increases the susceptibility of an area to debris flow.

The debris flow susceptibility map developed in this study identifies the factors causing debris flow and the locations susceptible to these events. In these locations, the barren expanse between the plantations can be turfed with grass or riveted for the prevention of movement and moisture control. Good land management practices in the plantations and cropland, and healthy irrigation practices can effectively reduce debris flow incidences in the study area. The map can assist road planners, land use managers, and agriculturists in their ventures toward development.

Acknowledgements This study was supported by DST-SERB under fast track scheme (No. SR/FTP/ETA-0062/2011). The authors would like to acknowledge with thanks, the financial support rendered by DST for the research.

References

Aleotti P, Chowdhury R (1999). Landslide hazard assessment: summary, review, and new perspectives. Bull Eng Geol Environ, 58(1): 21–44

Althuwaynee O F, Pradhan B, Ahmad N (2015). Estimation of rainfall threshold and its use in landslide hazard mapping of Kuala Lumpur metropolitan and surrounding areas. Landslides, 12(5): 861–875

Blahut J, van Westen J, Sterlacchini S (2010). Analysis of landslide inventories for accurate prediction of debris flow source areas. Geomorphology, 119(1–2): 36–51

Bregoli F, Medina V, Chevalier G, Hürlimann M, Bateman A (2015). Debris-flow susceptibility assessment at regional scale: validation on an alpine environment. Landslides, 12(3): 437–454

Chen J, Li Y, Zhou W, Iqbal J, Cui Z (2017). Debris-flow susceptibility assessment model and its application in semiarid mountainous areas of the southeastern Tibetan Plateau. Nat Hazards Rev, 18(2): 05016005

Cruden D M, Varnes D J, eds. (1996). Landslide types and processes. Landslides Investigations and Mitigation. In: Turner A K, Schuster R L, eds. National Research Council, Transportation Research Board, Washington DC, 36–75

Dai F C, Lee F C (2002). Landslide characteristics and slope instability modeling using GIS, Lantau Island, Hong Kong. Geomorphology, 42 (3–4): 213–228

D'Ambrosio D, Spataro W, Iovine G (2006). Parallel genetic algorithms for optimizing cellular automata models of natural complex phenomena: an application to debris-flows. Comput Geosci, 32(7): 861–875

Elkadiri R, Sultan M, Youssef A M, Elbayoumi T, Chase R, Bulkhi A B, Al-Katheeri M (2014). A remote sensing-based approach for debris-flow susceptibility assessment using artificial neural networks and logistic regression modeling. IEEE Journal of Selected Topics in Applied Earth Observations and Remote Sensing, 7(12): 4818–4835

Fell R, Corominas J, Bonnard C, Cascini L, Leroi E, Savage W Z (2008). Guidelines for landslide susceptibility, hazard, and risk zoning for land use planning. Eng Geol, 102(3–4): 85–98

Franks C A M (1999). Characteristics of some rainfall-induced landslides on natural slopes, Lantau Islands, Hong Kong. Q J Eng Geol, 32(3): 247–259

Gabet E J, Mudd S M (2006). Mobilization of Debris flow from shallow landslides. Geomorphology, 74(1–4): 207–218

Guzzetti F, Reichenbach P, Ardizzone F, Cardinali M, Galli M (2006). Estimating the quality of landslide susceptibility models. Geomorphology, 81(1–2): 166–184

Hungr O, Morgan G C, Kellerhals R (1984). Quantitative analysis of debris torrent hazards for design of remedial measures. Can Geotech J, 21(4): 663–677

Hürlimann M, Rickenmann D, Medina V, Bateman A (2008). Evaluation of approaches to calculate debris-flow parameters for hazard assessment. Eng Geol, 102(3–4): 152–163

IS: 2720-2006 Compendium of Soil Testing. Bureau of Indian Standards. New Delhi

Iverson R M (2000). Landslide triggering by rain infiltration. Water Resour Res, 36(7): 1897–1910

Iverson R M (2005). Regulation of landslide motion by dilatancy and pore-pressure feedback. J Geophys Res, 110(F2): F02015

Iverson N R, Mann J E, Iverson R M (2010). Effects of soil aggregates on debris-flow mobilization: Results from ring-shear experiments. Eng Geol, 114(1–2): 84–92

Keefer D K, Larsen M C (2007). Geology. Assessing landslide hazards. Science, 316(5828): 1136–1138

Kondratyev K Y, Krapivin V F, Varotsos C A (2006). Natural disasters as interactive components of global-ecodynamics. Springer/Praxis, Chichester, 625

Lee S, Ryu J H, Min K, Won J S (2003). Landslide susceptibility analysis using GIS and artificial neural network. Earth Surf Process Landf, 28 (12): 1361–1376

Liang W, Zhuang D, Jiang D, Pan J, Ren H (2012). Assessment of debris flow hazards using a Bayesian Network. Geomorphology, 171–172: 94–100

Lucà F, D'Ambrosio D, Robustelli G, Rongo R, Spataro W (2014). Integrating geomorphology, statistic, and numerical simulations for landslide invasion hazard scenarios mapping: an example in the Sorrento Peninsula (Italy). Comput Geosci, 67: 163–172

McMillan P, Brown D J, Forster A, Winter M G (2005). Debris flow information sources. In: Winter M G, Macgregor F, Shackman L, eds. Scottish Road Network Landslides Study. Edinburgh: The Scottish Executive, 25–44

Montgomery D R, Dietrich W E (1994). A physically-based model for the topographic control on shallow landsliding. Water Resour Res, 30 (4): 1153–1171

Neaupane K M, Piantanakulchai M (2006). Analytical network model for landslide hazard zonation. Eng Geol, 85(3–4): 281–294

Okano K, Suwa H, Kanno T (2012). Characterization of debris flows by rainstorm condition at a torrent on the Mount Yakedake Volcano, Japan. Geomorphology, 136(1): 88–94

Quan Luna B, Blahut J, van Westen C J, Sterlacchini S, Van Asch T W J, Akbas O (2011). The application of numerical debris flow modelling

for the generation of physical vulnerability curves. Nat Hazards Earth Syst Sci, 11(7): 2047–2060

Rickenmann D (1999). Empirical relationships for debris flow. Nat Hazards, 19(1): 47–77

Saaty T L (1980). The Analytic Hierarchy Process. New York: McGraw-Hill, 287

Santacana N, Baeza B, Corominas J, De Paz A, Marturiá J (2003). A GIS-based multivariate statistical analysis for shallow landslide susceptibility mapping in La Pobla de Lillet Area (Eastern Pyrenees, Spain). Nat Hazards, 30(3): 281–295

Shieh C L, Chen Y S, Tsai Y J, Wu J H (2009). Variability in rainfall threshold for debris flow after the Chi-Chi earthquake in central Taiwan, China. Int J Sediment Res, 24(2): 177–188

Sujatha E R, Sridhar V (2017). Mapping debris flow susceptibility using Analytical Network Process in Kodaikkanal Hills, Tamil Nadu (India). J Earth Syst Sci, 126(8): 116

Sujatja E R, Sruthi N (2016). Application of earned value management to compute the project performance using Analytical Network Process. Jordan Journal of Civil Engineering, 10(2): 254–265

van Westen C J, van Asch T W J, Soeters R (2006). Landslide hazard and risk zonation—why is it still so difficult? Bull Eng Geol Environ, 65 (2): 167–184

Vanacker V, Vanderschaeghe M, Govers G, Willems E, Poesen J, Deckers J, De Bievre B (2003). Linking hydrological, infinite slope stability and land-use change models through GIS for assessing the impact of deforestation on slope stability in high Andean watersheds. Geomorphology, 52(3–4): 299–315

Varnes D J (1984). Landslide Hazard Zonation: a review of principles and practice. In: IAEG Commission on Landslides, Paris

Winter M G (2013). DS 4.4 Lead discussion: landslides. In: Geotechnics of Hard Soils—Weak Rocks: Proceedings, 15th European Conference on Soil Mechanics and Geotechnical Engineering, Athens, Greece (Anagnostopoulos A, Pachakis M and Tsatsanifos C, eds. Amsterdam: IOS Press